Translational Oncology 43 (2024) 101911

Contents lists available at ScienceDirect

Translational Oncology

journal homepage: www.elsevier.com/locate/tranon

Original Research

Polyene phosphatidylcholine enhances the therapeutic response of oxaliplatin in gastric cancer through Nrf2/HMOX1 mediated ferroptosis

Peijie Lei [a,b,1], Lianjing Cao [a,1], Hongjun Zhang [a], Jialei Fu [a], Xiaojuan Wei [a], Fei Zhou [a], Jingjing Cheng [a], Jie Ming [a], Haijun Lu [a,*], Tao Jiang [a,*]

[a] Department of Radiation Oncology, The Affiliated Hospital of Qingdao University, Qingdao 266000, China
[b] Department of Medicine, Qingdao University, Qingdao 266000, China

ARTICLE INFO

Keywords:
Gastric cancer
Polyene phosphatidylcholine
Ferroptosis
Oxaliplatin

ABSTRACT

Oxaliplatin (OXA)-based chemotherapy is one of the first-line treatments for advanced gastric cancer. However, the potential risk for chemotherapy-induced hepatic injury can hinder its effectiveness. Polyene phosphatidylcholine (PPC) is often used as a hepatoprotective agent to counter OXA-induced hepatic injury; however, its impact on the antitumour effectiveness of OXA remains uncertain. Our retrospective study examined 98 patients with stage IV gastric cancer to assess the impact of PPC on progression-free survival (PFS) and disease control rate (DCR). Furthermore, *in vitro* and *in vivo* assays were conducted to elucidate the combined biological effects of OXA and PPC (OXA+PPC) on gastric cancer. RNA sequencing, luciferase reporter assays, live/dead cell assays, immunofluorescence, and western blotting were used to identify the activated signalling pathways and downstream factors post OXA+PPC treatment. The findings indicated that PPC served as an independent prognostic factor, correlating with prolonged PFS and improved DCR in patients with gastric cancer. The combination of OXA and PPC significantly inhibited tumour cell growth both *in vitro* and *in vivo*. RNA sequencing revealed that OXA+PPC treatment amplified reactive oxygen species and ferroptosis signalling pathways. Mechanistically, OXA+PPC upregulated the expression of haem oxygenase-1 by promoting the nuclear migration of nuclear factor erythroid 2-related factor (Nrf2), thereby enhancing its transcriptional activity. Drug-molecule docking analysis demonstrated that PPC competitively bound to the peptide structural domains of both Nrf2 and Kelch-like ECH-associated protein 1 (KEAP1), accounting for the increased translocation of Nrf2. In conclusion, our study reveals the synergistic antitumour potential of PPC and OXA while protecting patients against hepatic injury. This suggests a promising combined treatment approach for patients with advanced gastric cancer.

Introduction

Gastric cancer is the fifth most common cancer and the third leading cause of cancer-related deaths globally [1]. When diagnosed at an early stage, surgery is an effective treatment strategy; however, most patients are diagnosed at an advanced stage requiring chemotherapy [2]. Although novel anticancer drugs have enhanced the efficacy of chemotherapy, not all patients benefit from these advancements. As a result, the overall prognosis for individuals with gastric cancer remains suboptimal. Consequently, there is an urgent need for the development of chemotherapeutic sensitizers and reversal agents.

In the clinical treatment of tumours, a variety of chemotherapeutic drugs can induce liver injury, particularly platinum-containing agents like oxaliplatin (OXA), cisplatin, and carboplatin [3]. These drugs elicit liver cell injury and apoptosis through pathways involving oxidative stress and inflammatory responses, ultimately impacting liver function [4]. Polyene phosphatidylcholine (PPC) has demonstrated noteworthy efficacy and potential hepatoprotective effects in the management of chemotherapy patients with compromised liver function [5]. Our previous study showed that PPC and OXA combined treatment significantly reduced gastric cancer cell viability [6]. PPC is a primary component of essential phospholipids and is a non-toxic phospholipid rich in polyunsaturated fatty acids. It enhances membrane function and fluidity owing to its high affinity for membranes [7]. PPC has been shown to possess hepatoprotective properties, attributed to its antioxidant and free radical-neutralizing capabilities [8].

* Corresponding authors.
E-mail addresses: Lhj82920608@163.com (H. Lu), jiangtao111@qdu.edu.cn (T. Jiang).
[1] These authors contributed equally to this work.

https://doi.org/10.1016/j.tranon.2024.101911
Received 15 January 2024; Received in revised form 7 February 2024; Accepted 9 February 2024

Reactive oxygen species (ROS) are pivotal for various cellular functions. However, ROS dysregulation is frequently observed in cancer cells. Past studies highlighted the dual pro-tumour and anticancer roles of ROS in tumour regulation [9]. Notably, ROS influences epigenetic gene expression by either regulating the activities of DNA methyltransferase (DNMT) and histone deacetylase (HDAC) or causing hypomethylation through oxidative DNA damage [10]. Depending on the context, ROS can either promote oncogenic transformation or counteract tumour formation. Increased ROS levels can suppress tumours through various mechanisms including triggering tumour cell senescence and ferroptosis [11]. Clinically, PPC is often administered concomitantly with chemotherapy as a hepatoprotective agent. However, the potential impact of PPC on the antitumour efficacy of combined chemotherapy remains unclear. There is a dire need to address this knowledge gap to ensure that effective treatment is being provided to patients with cancer. Therefore, the aim of this study was to explore the impact of combined OXA and PPC chemotherapy on patients with gastric cancer. Furthermore, our goal was to determine whether PPC had a beneficial or negative impact on the efficacy of OXA in these patients, and to identify the underlying mechanisms involved.

In this study, we found a correlation between the co-administration of PPC and OXA with extended progression-free survival (PFS) and improved disease control rate (DCR) in patients with gastric cancer. Mechanistic studies showed that the combined use of PPC and OXA effectively competed with nuclear factor erythroid 2-related factor (Nrf2) to bind to the peptide structural domain of Kelch-like ECH-associated protein 1 (KEAP1). This interaction boosted the nuclear migration of Nrf2, subsequently amplifying the transcriptional activity of haem oxygenase-1 (HMOX1). Notably, the heightened HMOX1 activity resulted in an increased production of ROS, further inducing ferroptosis in gastric cancer cells.

Materials and methods

Patient recruitment and data compilation

We retrospectively enrolled 98 patients diagnosed with pathologically confirmed stage IV gastric adenocarcinoma at the Affiliated Hospital of Qingdao University from January 2015 to December 2016. The pathological diagnosis and clinicopathological staging were based on the World Health Organization (WHO) histological classification and the tumour-node-metastasis (TNM) classification system as outlined by the American Joint Committee on Cancer (AJCC) (1977). All patients underwent standard chemotherapy treatments: either OXA with teggio (SOX) or OXA combined with capecitabine (XELOX). We documented essential clinical parameters and whether PPC was used. Patients presenting with hepatic insufficiency before treatment or those exhibiting severe liver injury (grade 2 or higher) after one or two chemotherapy cycles were administered PPC. The liver injury grading was based on the Common Terminology Criteria for Adverse Events (CTCAE) version 5.0 (Supplementary Table 1). All patients provided informed consent, and the Research Ethics Committee of Qingdao University approved the utilization of the clinical and pathological data.

Cell lines and culture conditions

Human gastric cancer cell lines, AGS and HGC-27, were sourced from the Chinese Academy of Sciences (Shanghai, China). Foetal bovine serum (FBS) and Ham's F-12 K/RPMI-1640 medium were procured from Gibco (Thermo Fisher Scientific, Waltham, MA, USA). Cells were cultured in Ham's F-12 K and RPMI-1640 medium, supplemented with 10% FBS, 100 U/mL streptomycin, and 100 U/mL penicillin. Cells were incubated at 37 °C in a humidified chamber with 5% CO_2.

Cell growth and viability assays

Cell growth and viability assays were performed using the Cell Counting Kit-8 (CCK-8; Solarbio Science & Technology Co., Ltd., Beijing, China). The CCK-8 assay was performed as previously described [12]. Cells were seeded in 96-well plates at a density of 8000 cells/well. Following an 8 h attachment phase, cells were treated with either 20 μM OXA or 20 μM OXA and 16 μM PPC (OXA+PPC). Cell viability was assessed at 24, 36, 48, and 72 h using the CCK-8 assay. The colony formation assay was performed as described previously [13]. Briefly, 500 gastric cancer cells treated with OXA or OXA+PPC were seeded into 6-well plates and cultured for 14 d. Subsequently, the cells were fixed with 100% methanol, stained with crystal violet, and colonies with more than 50 cells were quantified. To identify the primary form of cell death induced by the combination treatment, inhibitors of various cell death mechanisms were introduced to the cells. The CCK-8 assay was then performed for cell viability measurement. The apoptosis inhibitor Z-VAD-FMK, programmed necrosis inhibitor necrostatin-1 (Nec-1), ferroptosis inhibitor Fer-1, and N-acetyl-L-cysteine (NAC) were purchased from MedChemExpress Co., Ltd. (Shanghai, China).

Western blotting

Whole cell lysates from treated AGS and HGC-27 cells were prepared and subjected to sodium dodecyl sulphate-polyacrylamide gel electrophoresis. Western blotting was carried out as previously described [14], using specific antibodies, including the Ferroptosis Antibody Sampler Kit (#29,650; Cell Signalling Technology, Danvers, MA, USA), haem Oxygenase 1 (sc-136,960; Santa Cruz Biotechnology, Dallas, TX, USA), β-actin (D16H11; Cell Signalling Technology), and Lamin B1 (12, 987–1-AP; Proteintech, Rosemont, IL, USA). The blots were visualized using the ECL Plus Western Blotting Detection System (GE Healthcare, Piscataway, NJ, USA) and analysed using the FluorChem Q imaging system (Alpha Innotech, San Jose, CA, USA).

Live and dead cell assays

A Calcein-AM/PI Double Stain Kit (40747ES76; Yeasen Biotechnology, Shanghai, China) was used to distinguish between live and dead cells. The calcein-AM dye penetrates live cell membranes and transforms into a green fluorescent form through the action of intracellular esterases. In contrast, the PI dye can only enter the membranes of dead cells, binding to nucleic acids to produce red fluorescence [15]. Briefly, cells were rinsed once with the appropriate medium, then resuspended in a serum-free medium. A combination of calcein-AM and PI dyes was added to the cell suspension. Following a 15-min incubation at 37 °C, the cells were visualized under a fluorescence microscope to differentiate between live cells (exhibiting green fluorescence) and dead cells (displaying red fluorescence).

Gastric cancer model and treatment in vivo

To assess the combined antitumour efficacy of OXA with PPC, female BALB/c nude mice (aged 5–6 weeks) were obtained from Beijing Vital River Laboratory Animal Technology Co., Ltd. (Beijing, China). HGC-27 cells (1×10^6) were subcutaneously injected into the right flank of each mouse. OXA and PPC were sourced from Jiangsu Hengrui Medicine Co., Ltd. (Jiangsu, China) and Chengdu Tiantaishan Pharmaceutical Co., Ltd. (Sichuan, China), respectively. OXA was prepared in dimethyl sulfoxide to the desired concentrations. Once the average tumour size reached approximately 100 mm^3, the mice were randomly categorized into the following treatment groups: control (phosphate buffered saline; PBS); 10 mg/kg OXA alone, administered intraperitoneally every 3 days; or combined OXA+PPC, where 30 mg/kg PPC was administered daily and 10 mg/kg OXA was administered every 3 days. Tumour dimensions were recorded thrice weekly using callipers, and volumes calculated using the

formula: $V = \text{length} \times \text{width}^2 \times 0.5$. Additionally, mouse weights were recorded bi-weekly. After a 3-week treatment period, the mice were humanely euthanized through cervical dislocation. Subsequently, the tumours were excised, embedded in paraffin, and sectioned. The extracted tumour samples were then stained with haematoxylin & eosin (H&E) for analysis. This study received approval from the Qingdao University's Institutional Animal Care and Use Committee.

Immunohistochemistry (IHC)

Immunohistochemical staining was performed on mice tumour tissues using antibodies against HMOX1 (sc-136,960; Santa Cruz Biotechnology) and Nrf2 (GB113808–100; Servicebio, Hubei, China). The tissues were fixed in formalin, embedded in paraffin, sectioned, and stored for further use. Prior to subsequent analyses, paraffin-embedded sections underwent deparaffinization and rehydration. Antigen retrieval was achieved by treating the sections in a pressure cooker for 2.5 min at a temperature just below boiling point. This was followed by a 10-min treatment with 3% H_2O_2 at room temperature. The sections were then incubated with primary antibodies overnight at 4 °C and subsequently with secondary antibodies (G1213–100UL; Servicebio) for 1 h at room temperature. Chromogenic detection was carried out by incubating with DAB for 7 min, followed by counterstaining using H&E, following standard protocols.

Quantitative real-time PCR (qRT-PCR)

Total RNA was extracted from mice tumour tissues and gastric cancer cells using TRIzol reagent (Life Technologies, Carlsbad, CA, USA), according to the manufacturer's instructions. Total RNA was quantified using a NanoDrop Spectrophotometer (Thermo Fisher Scientific). The RNA was then reverse transcribed using the PrimeScript RT Reagent Kit with gDNA Eraser (Takara, Japan), according to the manufacturer's instructions. qRT-PCR was performed using the LightCycler 480 SYBR Green I Master (Roche, Switzerland) in a 20 μL reaction mixture that included 10 ng cDNA and 250 nM of each primer. The thermal cycling conditions on the LightCycler480 Instrument II were set as: 95 °C for 10 min, followed by 40 cycles of 95 °C for 15 s, and 60 °C for 1 min. Primers specific to HMOX1 and β-actin were utilized as previously described [16].

Determination of ROS in vitro

AGS and HGC-27 cells were cultured and resuspended in Ham's F-12 K and RPMI-1640 medium, supplemented with 10% FBS, at a final cell density of 0.7×10^6 cells/mL. Samples were meticulously inspected for cell aggregation before being divided into control and treatment groups. The control group was treated with 20 μM OXA, while the treatment group was treated with a combination of 20 μM OXA and 16 μM PPC. After incubating for 48 h, the cells were washed thrice with 0.01 mol/L PBS.

To evaluate ROS levels, the DCFH-DA method was utilized using a ROS assay kit (Solarbio Science & Technology Co., Ltd.). Briefly, 10 μM 2′,7′-dichlorofluorescin diacetate (DCFDA) was added to the cells and incubated for 30 min at 37 °C, adhering to the manufacturer's protocol. Fluorescence signal was detected using a confocal laser-scanning microscope.

Antioxidant activity measurement

In vitro superoxide dismutase (SOD) activity was assessed using the WST-1 assay (Nanjing Jiancheng Bioengineering Institute, Nanjing, China) as per the manufacturer's instructions. Reduced glutathione (GSH) content was determined using a kit (Nanjing Jiancheng Bioengineering Institute). As per the manufacturer's protocol, the test sample and requisite reagents were added, followed by an incubation for 30 min at 37 °C or 2 min at room temperature. Absorbence was measured at either 450 or 405 nm using a microplate reader.

The concentration of malondialdehyde (MDA) was determined *in vitro* using a kit from Nanjing Jiancheng Bioengineering Institute, which utilizes thiobarbituric acid (TBA) reactivity. The procedure was conducted as per the manufacturer's instructions, and specific details for MDA measurement were obtained from the provided protocols.

Ferrous ion determination in vitro

Ferrous ions were measured *in vitro* using the Cell Ferrous Iron Colorimetric Assay Kit (Elabscience Biotechnology Co., Ltd., Wuhan, China), based on the manufacturer's protocol. Briefly, a complex was formed by binding ferrous ions to a probe, which displays a strong absorption peak at 593 nm. The optical density of this complex linearly correlates with the concentration of ferrous ions within a specific range. The absorbence was measured at 593 nm using a microplate reader based on the standard spectrophotometric method for quantitative analysis.

Luciferase reporter assay

The luciferase reporter assay was conducted as previously described [17]. Briefly, cells were seeded at a density of 1×10^5 cells/well in 12-well plates. Cells were then treated with either OXA or OXA+PPC. Both groups were transfected with the ARE reporter plasmid and co-transfected with the internal control plasmid pRL-TK. After 24 h post-transfection, the luciferase activity in each well was quantified using the Dual-Luciferase Reporter Assay System (DL101–01; Vazyme, Nanjing, China), following the manufacturer's guidelines.

Drug molecular docking analysis

The molecular structure files for target proteins KEAP1 and Nrf2 were sourced from the PDB database (https://www1.rcsb.org/). The molecular structure for PPC was obtained from PubChem (https://pubchem.ncbi.nlm.nih.gov/). Operations such as water molecule removal and proto-ligand deletion on the target proteins were performed using PyMOL software (version 2.3.0). We employed the Chem3D software (version 2020) to optimize the conformation of the PPC small molecule. This process used molecular mechanics to achieve the most energetically favourable conformation.

Using the AutoDock Tools 1.5.6, the pre-processed target protein molecules underwent hydrogenation. Furthermore, the optimal conformations of both aspirin and sulfinpyrazone molecules, derived from molecular dynamics optimization, were hydrogenated and torsionally bonded. Molecular docking of the target protein and ligand molecules was performed using AutoDock Vina v.1.2.0, using a Lamarckian genetic algorithm with semiflexible docking.

Statistical analysis

All statistical evaluations were performed using SPSS software (version 20.0; IBM Corp., Armonk, NY, USA). Disease-free survival (DFS)/PFS was defined as the duration in which a patient with cancer did not observe any progression of the disease or any exacerbation of cancer-related symptoms post-treatment. The DCR was defined as the proportion of patients showing a complete response, partial response, or stable disease following specific therapeutic intervention. Cox proportional hazards regression analyses were performed to determine the hazard ratios (HRs) for potential risk factors using the backward elimination technique. Differences in mean values were assessed using unpaired two-tailed Student's *t*-tests. Bioinformatics analysis of transcriptome sequencing data was performed as described previously [18], with quality control, alignment, gene expression quantification, differential expression examination, and functional enrichment analysis

conducted utilizing the R software (version 4.2.1). A *P*-value below 0.05 was deemed statistically significant. To designate levels of significance, the following notations were adopted: $*P < 0.05$, $**P < 0.01$, $***P < 0.001$, and $****P < 0.0001$.

Results

Patient demographics and clinical characteristics

Table 1 presents the clinical characteristics of the 98 patients included in the study. Amongst them, 55 (56.1%) were male and 43 (43.9%) were female. A total of 51 (52.0%) patients were aged over 55 years. Upon diagnosis, 19 (19.4%) patients were identified as stage IVa, while 79 (80.6%) were categorized as stage IVb. Chemotherapy treatments included SOX and XELOX for 68 (69.4%) and 30 (30.6%) patients, respectively. Within the cohort, 46 (46.9%) patients received PPC treatment. Furthermore, 48 (49.0%) patients experienced a PFS exceeding 6 months. During the follow-up period, disease progression was observed in 25 patients.

PPC treatment enhanced PFS in patients with advanced gastric cancer

The univariate COX analysis highlighted a significant association between PPC treatment and 6-month PFS ($P = 0.047$). While the association was not statistically significant in the multivariate analysis, there was a noticeable trend towards extended PFS with PPC treatment ($P = 0.053$) (Table 2). Moreover, both univariate and multivariate analyses underscored a significant correlation between PPC treatment and DCR (univariate analysis, $P = 0.021$; multivariate analysis, $P = 0.044$) (Table 3). Kaplan–Meier PFS curves further illustrated that patients treated with PPC had prolonged PFS when compared to those who did not receive PPC treatment ($P = 0.063$) (Fig. 1A).

PPC enhanced cell death in vitro and boosted antitumour effects in vivo

To evaluate the combined effectiveness of OXA and PPC, we performed CCK-8 and colony formation assays *in vitro*. The concentration of OXA (20 μM) for the *in vitro* assay was chosen based on the Half-Maximal Inhibitory Concentration (IC50) of gastric cancer cells (Supplementary Fig. S1a). The dose-dependent concentration for the combined OXA (20 μM) and PPC (16 μM) was determined using a cell viability assay (Supplementary Fig. S1b). The results revealed that OXA+PPC treatment notably decreased cell survival (Fig. 1B) and colony formation (Fig. 1C) in AGS and HGC-27 cells compared to the OXA-only group. The live/dead cell assays further confirmed an increased number of dead AGS and HGC-27 cells post OXA+PPC treatment (Fig. 1D), indicating the combination's potentiation of cell death in gastric cancer.

In a subsequent *in vivo* evaluation using a subcutaneous tumour model in nude mice, we observed that both tumour volume and weight were markedly reduced in the OXA+PPC group compared to the control and OXA-only groups (Fig. 1E). Assessing the body weight of the xenografted mice, a weight decrease was evident post drug administration in the OXA group, with a slight decline in the OXA+PPC group. However, survival rates remained consistent across all groups, with no casualties observed (Fig. 1F). Collectively, these findings underscore the synergistic effect of PPC and OXA in suppressing tumour cell growth, both *in vitro* and *in vivo*.

Table 1
Patient characteristics.

Variables	Cases	%
Gender		
Male	55	56.1
Female	43	43.9
Age		
<55	47	48.0
≥55	51	52.0
Stage		
IVa	19	19.4
IVb	79	80.6
Lauren type		
Diffuse	60	61.2
intestinal	38	38.8
Tumour location		
Gastric body	13	13.3
Gastric cardia	35	35.7
Pyloru&Antrum	50	51.0
Chemotherapy		
SOX	68	69.4
XELOX	30	30.6
PPC		
YES	46	46.9
NO	52	53.1
PFS		
≥6M	48	49.0
<6M	50	51.0
Therapeutic evaluation		
DCR	73	74.5
PD	25	25.5

Abbreviations: PFS: progression-free survival; M: month; DCR, Disease control rate; PD: Progressive disease.

PPC and OXA synergistically activated ROS and ferroptosis signalling pathways

To investigate the mechanisms by which PPC enhances the inhibition of gastric cancer cell proliferation, we carried out RNA-seq transcriptome analyses on cells treated with either OXA alone or a combination of OXA and PPC. A total of 195 differentially expressed genes (DEGs) were identified between these treatments. To elucidate the specific pathways influenced by PPC, we employed Kyoto encyclopedia of Genes and Genomes (KEGG) and Gene Ontology (GO) enrichment analyses on the DEGs using R software with the clusterProfiler package. Our results revealed that the predominant pathways impacted by PPC included ROS and ferroptosis (Fig. 2A). Intriguingly, the GO enrichment analysis of the differential genes in both treatment groups highlighted pathways associated with oxidative stress and iron ion transport (Fig. 2B). These observations suggest that PPC enhances OXA's efficacy by modulating these specific pathways.

PPC and OXA combination elevated ROS and ferrous ion generation

To investigate the mechanism underlying PPC's cell growth inhibition, we assessed the levels of ROS and markers related to ferroptosis in both the OXA+PPC and OXA groups. Fig. 2C reveals that the ROS levels were notably elevated in the OXA+PPC group compared to the OXA group in AGS and HGC-27 cells, signifying an upregulation in ROS expression due to PPC.

To confirm the role of oxidative stress, we evaluated the levels of MDA and the activities of GSH and SOD; all of which are key oxidative stress indicators. The OXA+PPC group displayed a marked rise in MDA content (Fig. 2D) and diminished SOD and GSH activities (Fig. 2E,F) compared to the OXA group. This suggests that PPC induced oxidative stress in gastric cancer cells. Furthermore, PPC treatment significantly increased the Fe^{2+} level (Fig. 2G).

Combined OXA and PPC treatment enhanced antitumour efficacy in gastric cancer cells due to ferroptosis

To determine the specific form of cell death induced by the combined PPC and OXA treatment in gastric cancer cells, we explored various inhibitors targeting recognized cell death pathways. These included the apoptosis inhibitor Z-VAD-FMK, the programmed necrosis inhibitor Nec-1, and the ferroptosis inhibitor Fer-1. Notably, only Fer-1 succeeded in reversing the reduced survival rate of gastric cancer cells (Fig. 2H,I).

Table 2
The influence of PPC on PFS (6 month) after chemotherapy.

Patient Characteristics	Cases	Univariate analysis			Multivariate analysis		
		HR	95% CI	*p*	HR	95% CI	*p*
Gender							
Male	55	1			1		
Female	43	0.579	0.330–1.433	0.437	0.411	0.412–1.667	0.352
Age							
<55	47	1			1		
≥55	51	0.545	0.354–1.228	0.552	0.575	0.335–1.454	0.645
Stage							
IVa	19	1			1		
IVb	79	0.736	0.338–1.996	0.586	0.866	0.657–2.012	0.725
Lauren type							
Diffuse	60	1			1		
intestinal	38	1.323	0.746–2.364	0.833	1.401	0.619–2.116	0.443
tumour location							
Gastric body	13	1			1		
Gastric cardia	35	1.146	0.615–3.889	0.559	1.409	0.684–4.002	0.601
Pyloru&Antrum	50	1.332	0.656–4.332	0.651	1.432	0.766–4.449	0.697
Chemotherapy							
SOX	68	1			1		
XELOX	30	0.835	0.622–2.992	0.756	0.778	0.654–3.112	0.783
PPC							
YES	46	1				1	
NO	52	0.471	0.221–0.915	**0.047**	0.512	0.298–1.045	**0.053**

Abbreviations: HR, hazard ratio; CI, confidence interval.

Table 3
The influence of PPC on DCR after chemotherapy.

Patient Characteristics	Cases	Univariate analysis			Multivariate analysis		
		HR	95% CI	*p*	HR	95% CI	*p*
Gender							
Male	55	1			1		
Female	43	0.665	0.396–1.257	0.453	0.463	0.541–1.495	0.334
Age							
<55	47	1			1		
≥55	51	0.476	0.398–1.352	0.469	0.502	0.312–1.62	0.534
Stage							
IVa	19	1			1		
IVb	79	0.672	0.338–2.325	0.437	0.475	0.334–1.557	0.446
Lauren type							
Diffuse	60	1			1		
intestinal	38	1.74	0.456–4.223	0.649	1.531	0.558–3.997	0.576
tumour location							
Gastric body	13	1			1		
Gastric cardia	35	1.586	0.557–3.334	0.496	1.745	0.449–4.748	0.745
Pyloru&Antrum	50	2.354	0.704–5.988	0.224	2.112	0.668–5.709	0.562
Chemotherapy							
SOX	68	1			1		
XELOX	30	1.553	0.475–4.485	0.549	1.226	0.554–4.779	0.637
PPC							
YES	46	1			1		
NO	52	0.551	0.302–0.889	**0.021**	0.473	0.258–0.935	**0.044**

Abbreviations: HR, hazard ratio; CI, confidence interval.

In contrast, neither Z-VAD-FMK or Nec-1 affected the decreased survival triggered by PPC and OXA combination treatment (Fig. 2J,K). This showed that the combined PPC and OXA treatment primarily triggered ferroptosis, rather than apoptosis or programmed necrosis, in gastric cancer cells. To delve deeper into the mechanism underlying ferroptosis in this combined treatment, we utilized NAC to neutralize the elevated ROS levels. The results showed that NAC nearly fully restored the survival rate of gastric cancer cells, which had been effectively reduced by combined PPC and OXA treatment (Fig. 2L). These findings confirm that the combined action of PPC and OXA triggers ferroptosis in gastric cancer cells through ROS production.

PPC and OXA synergistically enhanced HMOX1 expression and promoted Nrf2 nuclear translocation

DEGs identified in our transcriptome analysis revealed a notable elevation in HMOX1 expression within the OXA+PPC group (Fig. 3A,B). To confirm these findings, we assessed HMOX1 mRNA and protein levels and observed a significant upregulation in the OXA+PPC group, corroborating with the transcriptome sequencing findings (Fig. 3C,D). Prior studies indicate that HMOX1 promotes oxidative stress and accelerates ferroptosis by metabolizing haemoglobin and glutathione through the Nrf2/HMOX1 pathway [19]. Further investigation into KEAP1 and Nrf2 expression after combined OXA+PPC treatment revealed no notable change in KEAP1 levels between the groups. Yet, there was a marked increase in the nuclear expression of Nrf2 with PPC

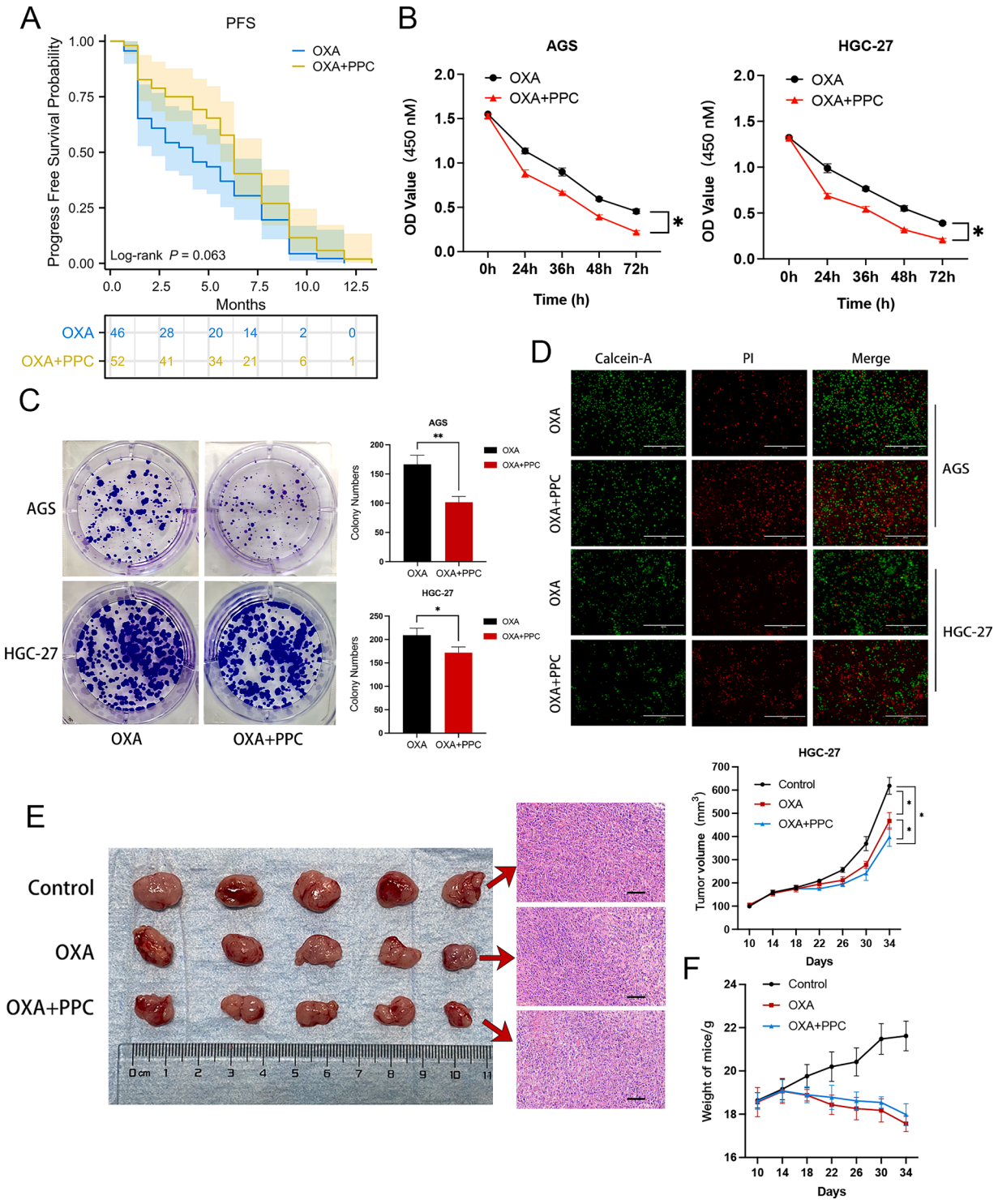

Fig. 1. Enhanced PFS and suppression of gastric cancer cell growth using combined PPC and OXA therapy. A Progression-free survival (PFS) comparison between patients with gastric cancer treated with and without PPC. B CCK-8 assay showing cell proliferation in AGS (left) and HGC-27 (right) cells, with and without PPC. C Evaluation of cell colony formation in the presence or absence of PPC, with quantification of colonies for each group. D Live/dead assay illustrating live (green) and dead (red) cells in the OXA group versus the OXA+PPC group over 24 h. Scale bar = 400 μm. E-F HGC-27 cells were introduced into nude mice ($n = 5$ per group). Upon reaching a tumour volume of 100 mm^3, mice received intraperitoneal injections of PBS and OXA (10 mg/kg), with or without PPC (30 mg/kg). Tumour dimensions and mouse weights were measured every 4 days, starting from the 10th day post-injection. Tumour tissues underwent haematoxylin and eosin staining for confirmation. Scale bar = 100 μm. Data are depicted as mean ± standard deviation (SD) (*$P < 0.05$, **$P < 0.01$, ***$P < 0.001$, ****$P < 0.0001$).

treatment (Fig. 3E,F). Immunofluorescence assays further supported this, indicating a significant surge of nuclear Nrf2 upon OXA+PPC treatment compared to the OXA-only group (Fig. 3G). Similarly, IHC analyses of mouse tumours displayed heightened expression of both Nrf2 and HMOX1 in the OXA+PPC group, with a distinct elevation of nuclear Nrf2 expression (Fig. 3H). Lastly, luciferase reporter gene assay results showed a significant increase in antioxidant response element (ARE) luciferase activity following combined OXA and PPC treatment

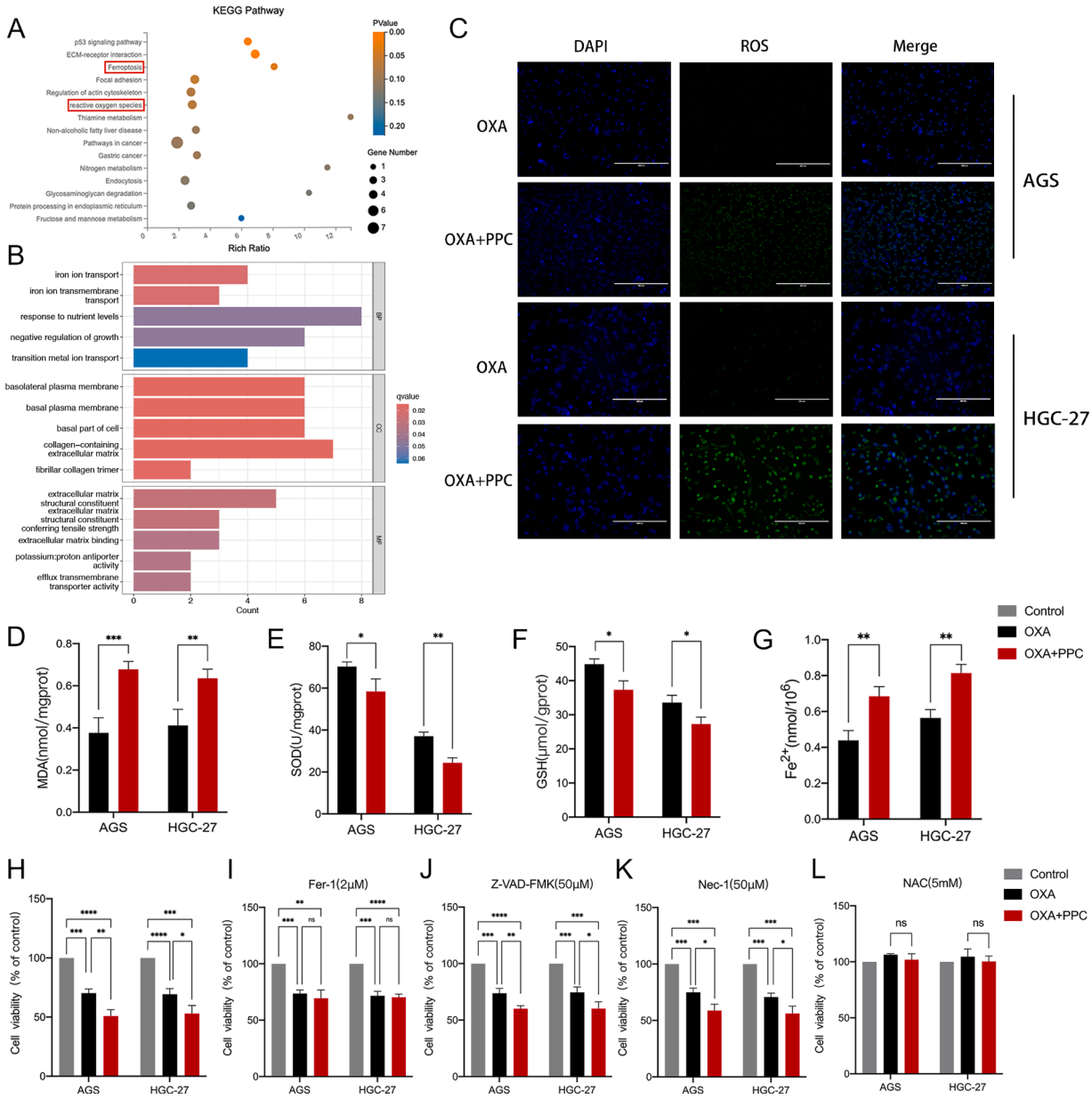

Fig. 2. PPC co-treatment induces oxidative stress and ferroptosis in gastric cancer cells. A-B KEGG and GO enrichment analyses of genes with significant differential expression between OXA+PPC and OXA-only treated cells, based on RNA-sequencing data. C ROS levels in gastric cancer cells post-treatment with or without PPC. Scale bar = 400 μm. D-G Evaluations of malondialdehyde (MDA) (D), superoxide dismutase (SOD) activity (E), glutathione (GSH) levels (F), and Fe^{2+} content (G) in gastric cancer cells treated with or without PPC. H-L Viability assessments of gastric cancer cells exposed to treatments with/without PPC for 24 h (H). Viability was also assessed in the presence of the ferroptosis inhibitor ferrostatin-1 (Fer-1; 2 μM) (I), the apoptosis inhibitor Z-VAD-FMK (50 μM) (J), the necroptosis inhibitor necrostatin (Nec-1; 50 μM) (K), and the antioxidant N-acetyl-L-cysteine (NAC; 5 mM) (L). Data are depicted as mean ± SD with significance indicators (*$P < 0.05$, **$P < 0.01$, ***$P < 0.001$, ****$P < 0.0001$).

(Fig. 3I). Overall, these findings clearly indicate that the OXA+PPC combination augments Nrf2 nuclear translocation and its transcriptional activity.

Competitive binding of PPC to the peptide structural domains of KEAP1 and Nrf2

Molecular docking analysis highlighted a strong interaction between PPC and KEAP1, with a docking score of −6.3 kcal/mol (Fig. 4A). This score suggests a significant binding affinity between the two molecules. A distinct alignment was evident when examining the peptide structural domains of KEAP1 and Nrf2 (Fig. 4B). In particular, the region where PPC binds to KEAP1 was closely aligned with the pocket region of Nrf2 on the KEAP1 target protein. Both these regions had a significant overlap in amino acid composition, namely AGR-415, AGR-418, TYR-334, and GLN-530. This overlap underscores the likelihood of PPC competitively binding to Nrf2's peptide structural domain.

Discussion

Chemotherapy is pivotal in the holistic treatment of advanced gastric cancer, often complemented by other modalities including surgery, radiation therapy, and immunotherapy [20–22]. It effectively manages tumour progression and metastasis, eases symptoms, and enhances overall treatment results and survival probabilities. However, despite advancements in chemotherapeutic approaches, the survival rates for

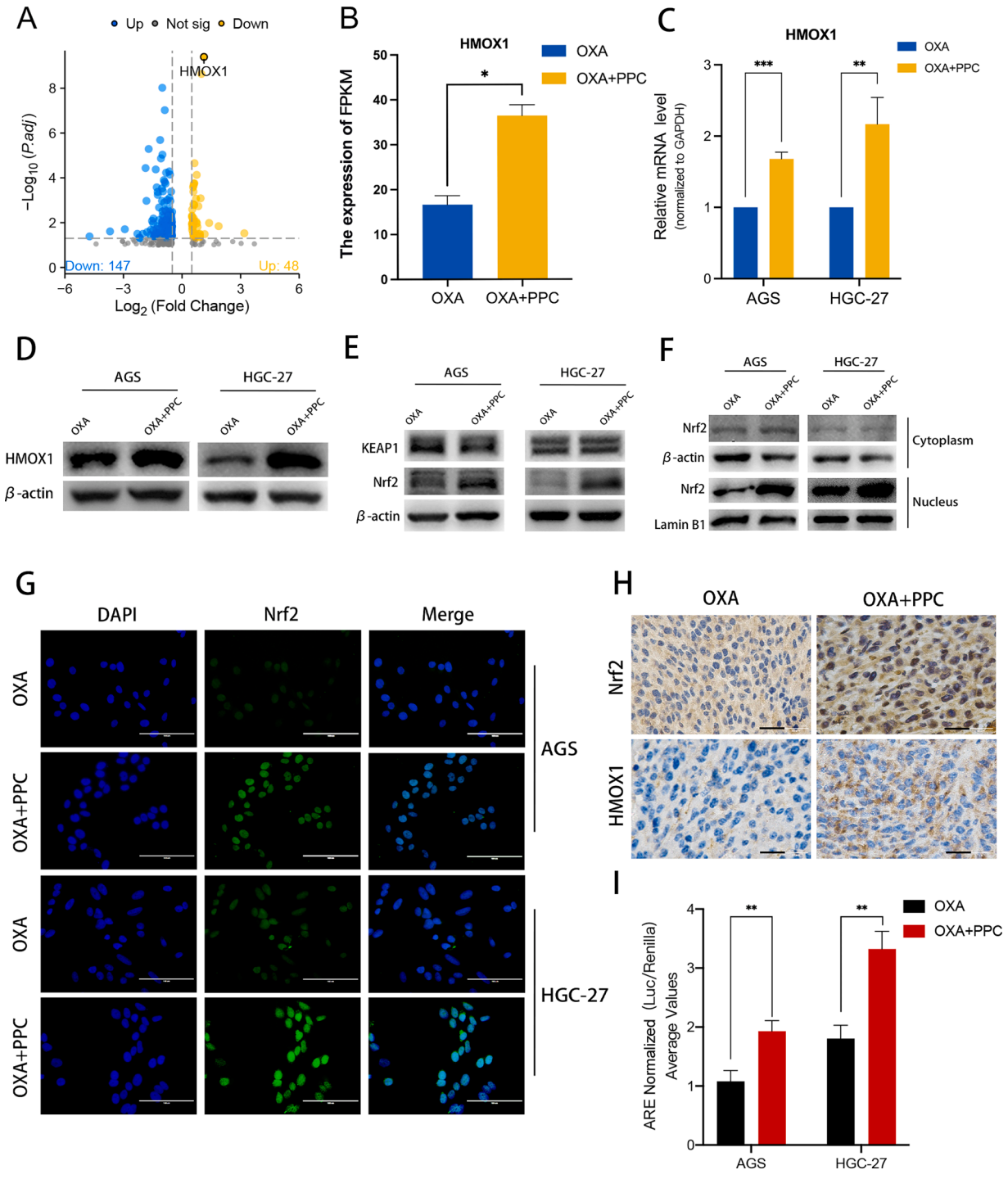

Fig. 3. OXA and PPC synergy activates the Nrf2/HMOX1 signalling pathway, amplifying HMOX1 gene expression. A RNA-sequencing was conducted to investigate expression differences in HGC-27 cells treated with and without PPC. Significantly altered genes following PPC treatment (log2FC > 2) are presented in the volcano plot. B-D RNA-sequencing data (B) highlighted a significant upregulation in HMOX1 expression upon combined OXA and PPC treatment. This observation was further supported by qRT-PCR (C) and western blotting (D) results. E The impact of OXA treatment on KEAP1 and Nrf2 expression, with or without PPC, evaluated through western blotting in AGS and HGC-27 cells using whole-cell lysates. F Influence of the combined treatment on AGS and HGC-27 cells analysed via western blotting, distinguishing between cytoplasmic and nuclear protein fractions. G Effect of the combined treatment on Nrf2 localization (green) and DAPI (blue) in AGS and HGC-27 cells visualized through immunofluorescence staining. Scale bar = 100 μm. H The impact of treatment, with or without PPC, on Nrf2 and HMOX1 expression examined using immunohistochemistry (IHC) on mouse tumour samples. Scale bar = 10 μm. I The combined treatment's modulation of the antioxidant response element (ARE) luciferase activity, with or without PPC, in AGS and HGC-27 cells.

patients with advanced gastric cancer remain disappointingly low. Furthermore, chemotherapy can lead to adverse effects that diminish a patient's quality of life. As a result, exploring innovative treatment methods, including targeted therapies, immunotherapies, and combined treatment plans, is essential to optimize outcomes for patients with gastric cancer [1].

PPC is a natural phospholipid primarily derived from soybeans or egg yolk [23]. Historically, PPC has been used clinically to treat liver

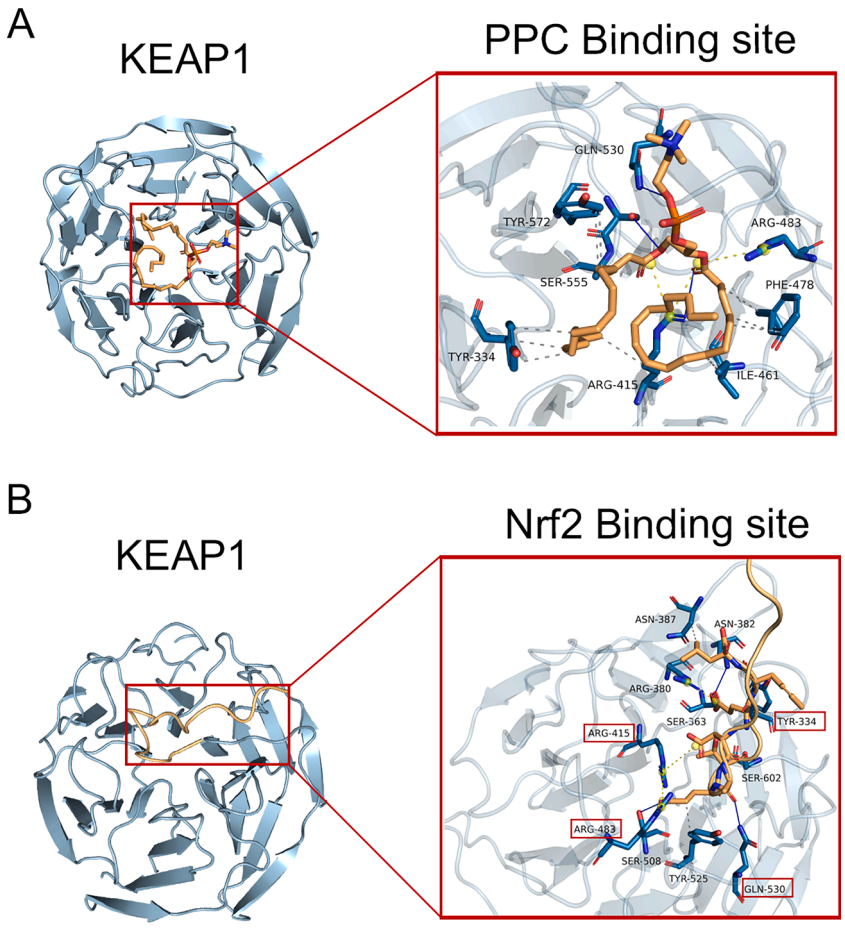

Fig. 4. PPC demonstrates competitive binding to the peptide domains of both KEAP1 and Nrf2. A Molecular docking analysis highlighting the interaction between PPC (orange) and KEAP1 (blue). B Docking analysis showcasing the interaction between Nrf2 (orange) and KEAP1 (blue). Grey dotted lines denote hydrophobic interactions, blue solid lines signify hydrogen bonds, and yellow dotted lines represent salt bridges. Amino acids within red boxes mark the consistent binding regions of both PPC and Nrf2 to the KEAP1 peptide.

conditions, including fatty liver, hepatitis B, and cirrhosis [24]. Recent studies have highlighted the antitumour properties of PPC, showcasing its ability to suppress tumour growth and metastasis via multiple pathways. Furthermore, PPC can enhance the effectiveness of chemotherapy and radiotherapy while diminishing their adverse effects [25]. Given its strong safety record and minimal side effects, PPC has garnered interest in the field of oncology; however, its role in cancer treatment remains inadequately explored.

Our current study demonstrates that PPC, in conjunction with OXA, enhances the effectiveness of chemotherapy on gastric cancer cells. Through transcriptome sequencing, we observed a marked increase in HMOX1 expression when using PPC and OXA together, compared to OXA alone. Consequently, we assessed HMOX1 expression in gastric cancer cell lines with and without PPC treatment. Using both qRT-PCR and western blotting, we found that HMOX1 expression, an enzyme that modulates intracellular haem metabolism, was notably elevated in the PPC-treated group. Its primary role is to facilitate the degradation of haem, leading to the production of carbon monoxide (CO), free iron ions, and bilirubin [26]. Both CO and bilirubin serve as biologically active metabolites, while the free iron ions participate in iron metabolism. Various factors, including oxidative stress, heat shock, cytokines, nutrients, and drugs, influence the expression of HMOX1. Altered HMOX1 expression is closely linked to the onset and progression of numerous conditions such as inflammation, tumours, and cardiovascular and neurodegenerative diseases [27,28]. HMOX1 is an inducible variant of haem oxygenase and reacts rapidly to stimuli such as oxidative stress, hypoxia, and inflammation. This has led to its recognition as an antioxidant and anti-apoptotic molecule [27,29]. Notably, elevated cellular HMOX1 levels are deemed to exert protective antioxidative properties against ROS [30]. However, it is also essential to understand that HMOX1 overexpression can exhibit pro-oxidant effects owing to its potential to generate ROS during haem breakdown, causing cellular damage and initiating apoptosis [31–33].

Activation of HMOX1 via the KEAP1-Nrf2 pathway is thought to play an oxidative role; oxidative agents might contribute to iron-dependent and oxidative cell death [19]. KEAP1, an E3 ubiquitin ligase, is vital in regulating NRF2 activity [34]. Typically, KEAP1 binds to NRF2 in the cytoplasm, leading to its ubiquitination and eventual proteasomal degradation, thus preventing the nuclear translocation of NRF2 [35]. However, when cells face oxidative stress or electrophilic compounds, ROS can alter cysteine residues on KEAP1, inducing a structural shift that interrupts KEAP1-NRF2 binding [36,37]. Consequently, NRF2 accumulates and translocates to the nucleus, binding with AREs and activating the transcription of downstream genes [38,39]. Moreover, KEAP1-NRF2 interaction can be disrupted by the phosphorylation of NRF2 by protein kinases, facilitating its dissociation from KEAP1 and allowing nuclear movement [39]. Therefore, the regulation of NRF2 is multifaceted, involving several pathways. Drug molecule docking revealed that PPC and Nrf2 have analogous pocket positions within KEAP1 target proteins, engaging mostly the same amino acids. This hints at a potential competitive interaction between the peptide structural domains of PPC and Nrf2. Experimental findings indicated that with PPC addition, the expression of KEAP1 in gastric cancer cells remained unchanged, while that of Nrf2 notably increased. This implies that PPC

elevates ROS levels in cells. This upregulation of ROS alters the binding dynamics between KEAP1 and Nrf2, impacting the ubiquitinated degradation of Nrf2. This results in an increased influx of Nrf2 into the nucleus and activates the downstream transcription of HMOX1. However, it is vital to recognize that HMOX1 overexpression can promote the expression of ROS, inducing oxidation, and excessive ROS production may induce ferroptosis.

Ferroptosis is a form of cell death characterized by membrane damage resulting from the production of lipid peroxides, which are formed through the oxidation of polyunsaturated fatty acids (PUFAs) on the lipid membrane. This oxidation occurs in the presence of iron ions and ROS [11]. Primarily, this process is driven by highly reactive hydroxyl radicals generated when ROS reacts with free ions, catalysing the oxidation of PUFAs and producing oxidized lipid peroxides. These peroxides can trigger a domino effect of free radicals on the membrane, causing oxidative damage, membrane disruption, and ultimately cell death [40,41]. Ferroptosis plays a crucial role in various conditions, including myocardial infarction, stroke, and neurodegenerative diseases. However, in the case of gastric cancer, it offers a potential therapeutic avenue [42]. Overexpression of HMOX1 results in the breakdown of haem into biliverdin, iron, and CO [43]. The iron liberated from this process can engage in reactions that either hinder the iron-recycling and storage pathways or stimulate the production of ferritin, a protein responsible for sequestering excess iron. Thus, HMOX1 overexpression culminates in the release of iron ions, influencing diverse aspects of cellular iron metabolism. The haem oxygenase reaction leads to the simultaneous release of substantial ROS and iron ions, which expedite the cellular oxidation of PUFAs on the lipid membrane, producing lipid peroxides. This cascade fosters ferroptosis in tumour cells.

This study provides compelling insights into the synergistic effects of PPC and OXA in treating gastric cancer, particularly through the Nrf2/HMOX1 pathway. However, there are some mechanistic limitations. Firstly, we observed an upregulation of HMOX1 expression in the PPC+OXA group, but we only validated the NrF2/ HMOX1 pathway reported in previous studies. Other potential signalling pathways remain to be explored. Secondly, although the molecular docking analysis reveals a strong interaction between PPC and KEAP1, it is essential to acknowledge that these results are computational predictions and are subject to limitations imposed by simulating static structures and the complex dynamics of biological environments. To address these constraints, further experimental validation is imperative, encompassing *in vitro* biophysical experiments, biochemical analyses, and cellular functional studies.

Based on our findings, we hypothesize that PPC may activate the Nrf2/HMOX1 pathway. An overexpression of HMOX1 can then potentially stimulate the ROS pathway, leading tumour cells to further produce ROS in large quantities. This can intensify cellular lipid peroxidation and promote ferroptosis in gastric cancer cells. Our findings underscore the pivotal role of PPC in enhancing the chemotherapeutic efficacy and promoting ferroptosis. In our study, the combination of OXA and PPC notably hindered proliferation and induced ferroptosis in both AGS and HGC-27 cells via the Nrf2/HMOX1 pathway. Additionally, when used together, PPC and OXA regulated intracellular iron balance by overexpressing HMOX1 in tumour cells. This resulted in a surge of intracellular ferrous iron content, amplifying cellular ferroptosis through oxidative stress activation. Furthermore, our *in vivo* studies confirmed that combining OXA with PPC markedly boosted the effectiveness of tumour treatment. Retrospective patient analyses also revealed that the OXA and PPC combination could enhance PFS and DCR while mitigating liver injury. Given these findings, our study holds significant clinical relevance. This study aimed to optimize therapeutic outcomes while minimizing hepatic-induced side effects and presents a novel strategy for advancing the understanding of PPC anticancer mechanisms and developing combined therapeutic approaches. In the future, further consideration should be given to the clinical translation of the study outcomes, introducing combination therapy into larger-scale clinical trials to verify its efficacy in patients with gastric cancer.

CRediT authorship contribution statement

Peijie Lei: Writing – original draft, Project administration, Methodology, Formal analysis, Data curation, Conceptualization, Validation. **Lianjing Cao:** Writing – review & editing, Methodology, Formal analysis, Conceptualization. **Hongjun Zhang:** Supervision, Investigation. **Jialei Fu:** Software, Investigation. **Xiaojuan Wei:** Software. **Fei Zhou:** Methodology. **Jingjing Cheng:** Validation. **Jie Ming:** Software. **Haijun Lu:** Supervision, Funding acquisition, Conceptualization. **Tao Jiang:** Writing – review & editing, Supervision, Resources, Methodology, Funding acquisition, Conceptualization.

Declaration of competing interest

The authors declare no conflict of interest in this study.

Supplementary materials

Supplementary material associated with this article can be found, in the online version, at doi:10.1016/j.tranon.2024.101911.

References

[1] E.C. Smyth, M. Nilsson, H.I. Grabsch, N.C. van Grieken, F. Lordick, Gastric cancer, Lancet 396 (2020) 635–648.
[2] W. Xue, B. Dong, Y. Wang, Y. Xie, P. Li, Z. Gong, Z. Niu, A novel prognostic index of stomach adenocarcinoma based on immunogenomic landscape analysis and immunotherapy options, Exp. Mol. Pathol. 128 (2022) 104832.
[3] F. Makowiec, S. Möhrle, H. Neeff, O. Drognitz, G. Illerhaus, O.G. Opitz, U.T. Hopt, A. zur Hausen, Chemotherapy, liver injury, and postoperative complications in colorectal liver metastases, J. Gastrointest. Surg. 15 (2011) 153–164.
[4] Y. Lu, S. Wu, B. Xiang, L. Li, Y. Lin, Curcumin attenuates oxaliplatin-induced liver injury and oxidative stress by activating the Nrf2 pathway, Drug Des. Dev. Ther. 14 (2020) 73–85.
[5] M. Li, Q. Luo, Y. Tao, X. Sun, C. Liu, Pharmacotherapies for drug-induced liver injury: a current literature review, Front. Pharmacol. 12 (2021) 806249.
[6] T. Jiang, H. Zhang, X. Liu, H. Song, R. Yao, J. Li, Y. Zhao, Effect of oxaliplatin combined with polyenephosphatidylcholine on the proliferation of human gastric cancer SGC-7901 cells, Oncol. Lett. 12 (2016) 4538–4546.
[7] H. Yu, Z. Yu, H. Huang, P. Li, Q. Tang, X. Wang, S. Shen, Gut microbiota signatures and lipids metabolism profiles by exposure to polyene phosphatidylcholine, Biofactors 45 (2019) 439–449.
[8] W. Okiyama, N. Tanaka, T. Nakajima, E. Tanaka, K. Kiyosawa, F.J. Gonzalez, T. Aoyama, Polyenephosphatidylcholine prevents alcoholic liver disease in PPARalpha-null mice through attenuation of increases in oxidative stress, J. Hepatol. 50 (2009) 1236–1246.
[9] E.C. Cheung, K.H. Vousden, The role of ROS in tumour development and progression, Nat. Rev. Cancer 22 (2022) 280–297.
[10] H.M. O'Hagan, W. Wang, S. Sen, C. Destefano Shields, S.S. Lee, Y.W. Zhang, E. G. Clements, Y. Cai, L. Van Neste, H. Easwaran, R.A. Casero, C.L. Sears, S.B. Baylin, Oxidative damage targets complexes containing DNA methyltransferases, SIRT1, and polycomb members to promoter CpG Islands, Cancer Cell 20 (2011) 606–619.
[11] X. Jiang, B.R. Stockwell, M. Conrad, Ferroptosis: mechanisms, biology and role in disease, Nat. Rev. Mol. Cell Biol. 22 (2021) 266–282.
[12] Y. Wang, Y. Xie, B. Dong, W. Xue, S. Chen, S. Mitsuo, H. Zou, Y. Feng, K. Ma, Q. Dong, J. Cao, C. Zhu, The TTYH3/MK5 positive feedback loop regulates tumor progression via GSK3-β/β-catenin signaling in HCC, Int. J. Biol. Sci. 18 (2022) 4053–4070.
[13] W. Xue, B. Dong, Y. Zhao, Y. Wang, C. Yang, Y. Xie, Z. Niu, C. Zhu, Upregulation of TTYH3 promotes epithelial-to-mesenchymal transition through Wnt/β-catenin signaling and inhibits apoptosis in cholangiocarcinoma, Cell. Oncol. (Dordr) 44 (2021) 1351–1361.
[14] L. Cao, F. Wang, S. Li, X. Wang, D. Huang, R. Jiang, PIM1 kinase promotes cell proliferation, metastasis and tumor growth of lung adenocarcinoma by potentiating the c-MET signaling pathway, Cancer Lett. 444 (2019) 116–126.
[15] P.N. Tawakoli, A. Al-Ahmad, W. Hoth-Hannig, M. Hannig, C. Hannig, Comparison of different live/dead stainings for detection and quantification of adherent microorganisms in the initial oral biofilm, Clin. Oral Investig. 17 (2013) 841–850.
[16] Y. Liu, P. Huang, Z. Li, C. Xu, H. Wang, B. Jia, A. Gong, M. Xu, Vitamin C sensitizes pancreatic cancer cells to erastin-induced ferroptosis by activating the AMPK/Nrf2/HMOX1 pathway, Oxid. Med. Cell. Longev. 2022 (2022) 5361241.
[17] L.J. Cao, Y.J. Zhang, S.Q. Dong, X.Z. Li, X.T. Tong, D. Chen, Z.Y. Wu, X.H. Zheng, W.Q. Xue, W.H. Jia, J.B. Zhang, ATAD2 interacts with C/EBPβ to promote esophageal squamous cell carcinoma metastasis via TGF-β1/Smad3 signaling, J. Exp. Clin. Cancer Res. 40 (2021) 109.

[18] W. Xue, K. Qiu, B. Dong, D. Guo, J. Fu, C. Zhu, Z. Niu, Disulfidptosis-associated long non-coding RNA signature predicts the prognosis, tumor microenvironment, and immunotherapy and chemotherapy options in colon adenocarcinoma, Cancer Cell Int. 23 (2023) 218.
[19] L.C. Chang, S.K. Chiang, S.E. Chen, Y.L. Yu, R.H. Chou, W.C. Chang, Heme oxygenase-1 mediates BAY 11-7085 induced ferroptosis, Cancer Lett. 416 (2018) 124–137.
[20] E.C. Smyth, Chemotherapy for resectable microsatellite instability-high gastric cancer? Lancet Oncol. 21 (2020) 204.
[21] J. Stiekema, A.K. Trip, E.P. Jansen, M.J. Aarts, H. Boot, A. Cats, O.B. Ponz, P. L. Gradowska, M. Verheij, J.W. van Sandick, Does adjuvant chemoradiotherapy improve the prognosis of gastric cancer after an r1 resection? Results from a dutch cohort study, Ann. Surg. Oncol. 22 (2015) 581–588.
[22] Y.K. Kang, N. Boku, T. Satoh, M.H. Ryu, Y. Chao, K. Kato, H.C. Chung, J.S. Chen, K. Muro, W.K. Kang, K.H. Yeh, T. Yoshikawa, S.C. Oh, L.Y. Bai, T. Tamura, K. W. Lee, Y. Hamamoto, J.G. Kim, K. Chin, D.Y. Oh, K. Minashi, J.Y. Cho, M. Tsuda, L.T. Chen, Nivolumab in patients with advanced gastric or gastro-oesophageal junction cancer refractory to, or intolerant of, at least two previous chemotherapy regimens (ONO-4538-12, ATTRACTION-2): a randomised, double-blind, placebo-controlled, phase 3 trial, Lancet 390 (2017) 2461–2471.
[23] J. Zhang, X. Zang, J. Lv, Y. Zhang, Z. Lv, M. Yu, Changes in Lipidomics, Metabolomics, and the Gut Microbiota in CDAA-Induced NAFLD Mice after polyene phosphatidylcholine treatment, Int. J. Mol. Sci. 24 (2023) 1502.
[24] Y. Li, A. Chen, Z. Li, X. Cui, G. Zhang, Effectiveness of polyene phosphatidylcholine and its combination with other drugs in patients with liver diseases based on real-world research, Expert Rev. Clin. Pharmacol. 15 (2022) 1363–1375.
[25] H. Zhang, T. Jiang, H. Yu, H. Lu, Y. Zhao, Y. Zhang, J. Fu, W. Chen, P. Dong, L. Zang, H. Song, Polyene phosphatidylcholine protects against radiation induced tissue injury without affecting radiotherapeutic efficacy in lung cancer, Am. J. Cancer Res. 9 (2019) 1091–1103.
[26] S.W. Ryter, A.M. Choi, Targeting heme oxygenase-1 and carbon monoxide for therapeutic modulation of inflammation, Transl. Res. 167 (2016) 7–34.
[27] A.L. Furfaro, N. Traverso, C. Domenicotti, S. Piras, L. Moretta, U.M. Marinari, M. A. Pronzato, M. Nitti, The Nrf2/HO-1 axis in cancer cell growth and chemoresistance, Oxid. Med. Cell. Longev. 2016 (2016) 1958174.
[28] S.W. Ryter, Heme oxygenase-1: an anti-inflammatory effector in cardiovascular, lung, and related metabolic disorders, Antioxidants (Basel) 11 (2022) 555.
[29] E. Amata, V. Pittalà, A. Marrazzo, C. Parenti, O. Prezzavento, E. Arena, S. M. Nabavi, L. Salerno, Role of the Nrf2/HO-1 axis in bronchopulmonary dysplasia and hyperoxic lung injuries, Clin. Sci. (Lond.) 131 (2017) 1701–1712.
[30] B. Wegiel, Z. Nemeth, M. Correa-Costa, A.C. Bulmer, L.E. Otterbein, Heme oxygenase-1: a metabolic nike, Antioxid. Redox Signal. 20 (2014) 1709–1722.
[31] N.J. Lamb, G.J. Quinlan, S. Mumby, T.W. Evans, J.M. Gutteridge, Haem oxygenase shows pro-oxidant activity in microsomal and cellular systems: implications for the release of low-molecular-mass iron, Biochem. J. 344 (Pt 1) (1999) 153–158.
[32] S.W. Ryter, R.M. Tyrrell, The heme synthesis and degradation pathways: role in oxidant sensitivity. Heme oxygenase has both pro- and antioxidant properties, Free Radic. Biol. Med. 28 (2000) 289–309.
[33] H. Zukor, W. Song, A. Liberman, J. Mui, H. Vali, C. Fillebeen, K. Pantopoulos, T. D. Wu, J.L. Guerquin-Kern, H.M. Schipper, HO-1-mediated macroautophagy: a mechanism for unregulated iron deposition in aging and degenerating neural tissues, J. Neurochem. 109 (2009) 776–791.
[34] M. Rojo de la Vega, E. Chapman, D.D. Zhang, NRF2 and the hallmarks of cancer, Cancer Cell 34 (2018) 21–43.
[35] S. Tao, P. Liu, G. Luo, M. Rojo de la Vega, H. Chen, T. Wu, J. Tillotson, E. Chapman, D.D. Zhang, p97 negatively regulates NRF2 by extracting ubiquitylated NRF2 from the KEAP1-CUL3 E3 complex, Mol. Cell. Biol. 37 (2017) e00660-16.
[36] L. Baird, D. Llères, S. Swift, A.T. Dinkova-Kostova, Regulatory flexibility in the Nrf2-mediated stress response is conferred by conformational cycling of the Keap1-Nrf2 protein complex, Proc. Natl. Acad. Sci. USA 110 (2013) 15259–15264.
[37] D.D. Zhang, M. Hannink, Distinct cysteine residues in Keap1 are required for Keap1-dependent ubiquitination of Nrf2 and for stabilization of Nrf2 by chemopreventive agents and oxidative stress, Mol. Cell. Biol. 23 (2003) 8137–8151.
[38] K. Itoh, J. Mimura, M. Yamamoto, Discovery of the negative regulator of Nrf2, Keap1: a historical overview, Antioxid. Redox Signal. 13 (2010) 1665–1678.
[39] P. Shaw, A. Chattopadhyay, Nrf2-ARE signaling in cellular protection: mechanism of action and the regulatory mechanisms, J. Cell. Physiol. 235 (2020) 3119–3130.
[40] G. Lei, L. Zhuang, B. Gan, Targeting ferroptosis as a vulnerability in cancer, Nat. Rev. Cancer 22 (2022) 381–396.
[41] A. Fischbacher, C. von Sonntag, T.C. Schmidt, Hydroxyl radical yields in the Fenton process under various pH, ligand concentrations and hydrogen peroxide/Fe(II) ratios, Chemosphere 182 (2017) 738–744.
[42] R. Gu, Y. Xia, P. Li, D. Zou, K. Lu, L. Ren, H. Zhang, Z. Sun, Ferroptosis and its role in gastric cancer, Front. Cell Dev. Biol. 10 (2022) 860344.
[43] L.R. Vasconcellos, F.F. Dutra, M.S. Siqueira, H.A. Paula-Neto, J. Dahan, E. Kiarely, L.A. Carneiro, M.T. Bozza, L.H. Travassos, Protein aggregation as a cellular response to oxidative stress induced by heme and iron, Proc. Natl. Acad. Sci. USA 113 (2016) E7474–e7482.